# Advances in targeted cancer imaging using galactose-modified polymeric nanoparticles: A systematic review

Mouzhan Rasoulianshiadehi[1], Tahereh Zadeh Mehrizi[2], Babak Eshrati[2,3], Mehdi Shafiee Ardestani[1]
[1]Department of Radiopharmacy, Faculty of Pharmacy, Tehran University of Medical Sciences, Tehran, Iran
[2]Vaccine Research Center, Iran University of Medical Sciences, Tehran, Iran
[3]Department of Community and Family Medicine, Faculty of Medicine, Iran University of Medical Sciences, Tehran, Iran

**Corresponding Author:**
Dr. Tahereh Zadeh Mehrizi
Address: Vaccine Research Center, Iran University of Medical Sciences, Tehran, Iran.
Email: taherehzadehmehrizi@gmail.com

**Running title:** Galactose-modified nanoparticles in cancer imaging

**Article History:**
Received: 23 June 2025
Revised: 16 November 2025
Accepted: 20 November 2025
Published Online: 27 December 2025

**ABSTRACT**
**Introduction:** Early cancer detection remains challenging due to the limited sensitivity and specificity of conventional imaging. Galactose-functionalized polymeric nanoparticles (Gal-PNPs) target galactose-recognizing receptors, such as asialoglycoprotein receptor (ASGPR) and galectins. This systematic review evaluated their design strategies, imaging efficacy, and biosafety across various cancer models.
**Methods:** Following PRISMA 2020 guidelines, PubMed, Web of Science, and Scopus were searched for English-language original research articles published between 2015 and 2025. Eligible studies included in vivo and ex vivo research employing Gal-PNPs for molecular imaging in cancer. Extracted data encompassed nanoparticle composition, galactosylation chemistry, imaging modality, receptor specificity, biodistribution, and safety outcomes. Given the heterogeneity of nanoparticle types and imaging platforms, a narrative synthesis was performed. The risk of bias was assessed using a modified SYRCLE tool.
**Results:** Twelve studies met the inclusion criteria. Gal-PNPs demonstrated strong performance across fluorescence, near-infrared, PET/CT, nuclear, and photothermal imaging. Most studies targeted hepatocellular carcinoma via ASGPR, while others explored galectin-mediated targeting in bladder, breast, and glioblastoma cancer models. Diverse galactosylation methods, click chemistry, amide coupling, ring opening, and metabolic glycoengineering were applied to

polymeric backbones such as dendrimers, chitosan, alginate, and micelles. Gal-PNPs achieved superior tumor selectivity, high tumor-to-background ratios, sustained signal retention, and favorable biocompatibility.
**Conclusion:** Gal-PNPs constitute a selective, biocompatible, and versatile platform for receptor-targeted cancer imaging. Their dual diagnostic and therapeutic potential, combined with molecular adaptability, highlights their translational promise in precision oncology. Future research should extend these systems to non-hepatic malignancies, standardize formulation characterization, and advance clinical imaging validation.

**Keywords:** Galactose; Molecular imaging; Polymeric nanoparticles; Neoplasms

## INTRODUCTION

Cancer remains a serious global health challenge and is currently the leading cause of death in many countries [1]. Accurate diagnosis of this disease plays a key role in improving patient prognosis and reducing mortality [2]. Although conventional imaging modalities continue to play an undeniable role in medical diagnosis, these techniques suffer from limited sensitivity, insufficient specificity, and low image resolution in the early stages of the disease [3, 4]. To address these limitations, the innovative convergence of nanotechnology and molecular imaging has opened up new horizons to improve diagnostic accuracy. This is due to the ability of nanocarriers to selectively identify tumor tissues through both active and passive targeting mechanisms [5-9].

Among various nanoparticles, polymer nanoparticles (PNPs) have attracted considerable attention due to their biocompatibility, structural flexibility, and versatility [10-12]. These features allow the design of nanoparticles that can persist in the circulatory system for a long time, exhibit controlled release, and simultaneously deliver diagnostic and therapeutic agents [6, 13]. In addition, significant advances in polymer chemistry and nanofabrication technology have enabled the fabrication of polymer nanoparticles sensitive to tumor-specific stimuli, such as low acidity, redox potential, or enzymatic activity, with high precision [14-16]. This intelligent feature improves the signal-to-noise ratio and increases imaging accuracy [12, 17].

Despite the significant advantages of multifunctional polymeric nanoparticles, several biological and transportability challenges have prevented their full clinical application. Rapid clearance of nanoparticles by the mononuclear phagocyte system (MPS), safety concerns, and the accelerated blood clearance (ABC) phenomenon all reduce the effective bioavailability and targeting efficiency of conventional nanosystems [18-20]. Despite their advantages in multimodal imaging, the use of inorganic components, such as gold nanoparticles, iron oxide nanoparticles, or quantum dots, may be associated with challenges such as increased toxicity, reduced biodegradability, and limitations in formulation design [21, 22]. These obstacles emphasize the need to develop novel targeting strategies that can enhance tumor tissue specificity, effectively evade immune recognition, and maintain biosafety, paving the way for safe and efficient application of nanoparticles in the clinical setting.

In this context, galactose-functionalized polymeric nanoparticles (Gal-PNPs) have been introduced as a new generation of receptor-targeted imaging probes that have great potential for advancing cancer diagnosis [23-34]. Galactose, as a natural monosaccharide, has a strong binding affinity for a set of carbohydrate-binding receptors that are abnormally overexpressed in many cancers [35]. In particular, the asialoglycoprotein receptor (ASGPR), which are predominantly expressed in normal liver cells as well as in hepatocellular carcinoma (HCC), along with the protein galectin-1, which plays a key role in tumor progression in glioblastoma, bladder cancer, and other solid tumors, are considered major targets in galactose-based recognition [36, 37]. The attachment of galactose ligands to the surface of polymeric nanocarriers has enabled the design of imaging probes that enter cells via receptor-dependent endocytosis, which leads to their selective accumulation in tumors, imaging specificity, and improved image resolution [23-34].

Beyond their targeting capabilities, Gal-PNPs are emerging as versatile platforms that can be coupled to a variety of imaging agents, such as fluorescent dyes (such as near-infrared fluorophores), radionuclides, and magnetic contrast agents [23-34]. This feature allows for the use of optical, nuclear, and magnetic resonance imaging modalities. Furthermore, the addition of environment-sensitive components, such as pH-sensitive ligands or redox-responsive systems, allows Gal-PNPs to activate imaging signals only under specific conditions of the tumor microenvironment [38-40]. This mechanism not only increases the accuracy of detection, but also reduces systemic background noise and improves imaging resolution [40].

Despite their significant potential, the existing studies on Gal-PNPs are still rare and heterogeneous, with a wide variety of design strategies, imaging targets, and preclinical models used. Therefore, this systematic and comprehensive evaluation was needed to integrate the available knowledge in this field, properly assess the clinical translational potential of these nanocarriers, and identify and address existing research gaps. Accordingly, the present systematic review aimed to comprehensively evaluate Gal-PNPs designed for precise cancer imaging.

## METHODS

### Search strategy

This study aimed to find out the impacts of galactosylated polymeric nanoparticles as receptor-based targeted molecular imaging agents on different cancers. For this purpose, a systematic review was done under the PRISMA 2020 guidelines [41]. Ethics approval was received from the ethics committee of Iran University of Medical Sciences (No: IR.IUMS.REC.1404.016).

A systematic literature search was conducted through PubMed, Web of Science, and Scopus databases. Our search scope was limited to peer-reviewed research articles published in English between 2015 and 2025. A combination of MeSH and non-MeSH terms was used, and the complete and reproducible search strategy is summarized in Table 1. Also, Boolean operators (AND/OR) were used to refine the results further. Duplicate records were removed, and titles and abstracts were reviewed based on their relevance to the topic. Articles that passed the initial screening stage were evaluated in full text.

### Study selection

The population was human, animal, and ex vivo cancer models. The intervention of interest was cancer targeting with Gal-PNPs for molecular imaging. These nanoparticles were used as carriers for common imaging agents. Comparison groups were not necessarily needed, but those studies in which nanoparticles without a galactose ligand were used were graded higher for review.

Only English-language original research papers that reported experimental results on cancer imaging using Gal-PNPs were considered for inclusion. Review articles, conference proceedings, studies without an imaging section, and those that investigated non-polymer-based nanoparticles or those without galactosylated modification were excluded from the final analysis. All included studies were independently reviewed by two authors. In cases of disagreement, a supervisor intervened to make the final decision.

**Data extraction and synthesis**

A standard form for data extraction was designed and developed in Microsoft Excel software that was applied to a pilot set of included studies to assess its validity before final implementation. The following information was extracted from the selected articles:

- ***Study characteristics:*** Authors' names, year of publication, country of study, type of cancer model, and tumor type.
- ***Nanoparticle composition:*** Polymer type, synthesis, and galactosylation method, particle size, surface charge, and physicochemical stability.
- ***Imaging method:*** Imaging agent, imaging modality (nuclear and radionuclide-based imaging, fluorescence, near-infrared, PET/CT, and photothermal imaging), imaging efficacy (e.g., tumor uptake, signal intensity in the tumor area, along with increased specificity and selectivity).
- ***Target receptor information:*** Receptor type and methods used to validate targeting.
- ***Biodistribution pattern and targeting efficiency:*** Accumulation in tumor tissue and extent of diffusion in non-target tissues.

Given the heterogeneity in nanoparticle formulations, imaging platforms, and models evaluated, data synthesis was performed in a narrative manner. Tables and graphs were used to categorize and compare studies by imaging modality and cancer type.

**Risk of bias assessment**

The risk of bias in individual studies was evaluated using the Systematic Review Centre for Laboratory Animal Experimentation (SYRCLE) Risk of Bias tool [42]. This instrument assesses ten domains: (i) sequence generation, (ii) baseline characteristics, (iii) allocation concealment, (iv) random housing, (v) blinding of caregivers, (vi) random outcome assessment, (vii) blinding of assessors, (viii) completeness of outcome data, (ix) selective outcome reporting, and (x) other potential biases. Each domain was rated as low, unclear, or high risk [42]. Visual summaries were generated using the ROBVIS tool.

## RESULTS

**Study selection**

The PRISMA flow diagram (Figure 1) describes the process of study selection. Accordingly, 161 articles were identified after a systematic search across PubMed (n=36), Web of Science (n=57), and Scopus (n=68) databases. After removing 63 duplicates, 98 studies were eligible for title and abstract screening. After initial screening, 20 articles were selected for full-text review. Of these, eight studies were excluded for the following reasons: in vitro design (n=3), non-polymeric nanoparticle formulations (n=2), focus on liver diseases rather than cancer (n=1), use of lectins instead of galactose (n=1), and absence of imaging outcomes (n=1). Finally, 12 studies met the inclusion criteria and were included in the analysis, comprising predominantly animal models (n=11) and one ex vivo study [23-34].

Table 2 represents Gal-PNPs targeting ASGPR in hepatic tumors, while Table 3 gives Gal-PNPs targeting Galectin or β-Galactosidase in the Tumor microenvironment.

**Targeted imaging of solid tumors**

This section is divided into two parts: “Different chemistry strategies for developing Gal-PNPs,” which explains the nanoparticle formulations, and “Imaging efficacy of Gal-PNPs,” which describes how well they work in different imaging methods.

### ***Different chemistry strategies for developing Gal-PNPs***

- *Dendrimer-based nanoprobes*

Yang et al. (2024) prepared dendritic Den@5F nanoprobes through a multistep chemical modification of the dendrimer-acetate core (Den-Acet). To prepare this formulation, Gal-PEG-$N_3$, $H_2N$-PEG-$N_3$, and Cy5-$N_3$ molecules were attached onto the dendrimer by a copper-catalyzed alkyne-azide click reaction (CuAAC). This reaction facilitated site-specific fluorescence emission and surface functionalization. Next, phenylboronic acid (PBA) and mNB (4-(4-(hydroxymethyl)-2-methoxy-5-nitrophenoxy)butanoate), as a photocrosslinking group, were introduced into the framework by an amide reaction with EDC/NHS activation. This biconjugation method allowed the nanoprobe to bind specifically to sialic acid residues overexpressed on the surface of tumor cells. When activated by UV light, the nanoprobe becomes stably immobilized at the tumor site. The chemical design in the study created "super-galactocations" upon stimulation by UV light, which greatly enhanced the delivery of galactose to the tumor surface [23].

In another study, Sharma et al. (2021) used fourth-generation hydroxyl-terminated poly(amidoamine) dendrimers (G4-PAMAM-OH) functionalized via a CuAAC click reaction to attach to monosaccharides such as β-D-galactose (D-GAL), β-D-glucose (D-GLU), and α-D-mannose (D-MAN) using a $PEG_4$ insoluble linker. After attachment of sugars, the dendrimers were labeled with the fluorescent dye Cy5, the presence of which was confirmed by distinct peaks in the NMR spectrum and optical absorption at 650 nm [33].

Pereira et al. (2020) also designed a dendritic nanoprobe via a dinucleophilic substitution reaction. This enabled the attachment of galactose units to the nanoparticle. For PET/CT imaging, $^{18}F$-fluoroethyl groups were then attached to the nanoprobe. These modifications increased the specificity of the nanoprobe for galectin-1, a carbohydrate-binding protein overexpressed in bladder cancer cells (a high binding affinity with a dissociation constant of $0.067 \pm 0.01$ mM) [32].

- *Hybrid polymer-based nanocarriers*

In a study, Ye et al. (2018) developed galactose-conjugated polymer micelles. These nanocarriers were constructed from cationic copolymers of poly(2-(dimethylamino)ethyl methacrylate) (PDMAEMA), which were labeled with rhodamine B (RhB) and branched with poly(3-azido-2-hydroxypropyl methacrylate) (PGMA-$N_3$), resulting in the formation of a core structure of RhB-PDMAEMA-c-PGMA. Subsequently, galactose was covalently bound to the nanosystem via a CuAAC reaction (RhB-PDMAEMA-c-PGMA-Gal). Among the different formulations, RhB-$PDMAEMA_{25}$-c-$PGMA_{50}$-Gal, known as Gal-micelles, exhibited the best physicochemical properties [28].

An et al. (2019) fabricated a galactose-based zwitterionic nanocarrier system with two amphiphilic block copolymers, including poly(2-O-acryloyloxyethyl-(2,3,4,6- β-D-galactopyranoside))-block-poly(2-(5,5-dimethyl-1,3-dioxan-2-yloxy)ethyl acrylate) (PGEA-b-PDMDEA) and poly(sulfobetaine methacrylate)-block-poly(2-(5,5-dimethyl-1,3-dioxan-2-yloxy)ethyl acrylate) (PSBMA-b-PDMDEA). PSBMA moieties created a zwitterionic coating to improve the colloidal stability of the formulation and reduce their nonspecific interactions with serum proteins [34].

- *ROS-responsive formula*

Liu et al. (2024) fabricated a smart galactose-fused prodrug, called FDROS-4, to detect ROS, such as hypochlorous acid (HOCl). In this nanodrug, 2,6-bis(hydroxymethyl)aniline (BHA) acted as an arylamine-based core that enabled ultrafast activation against ROS. This design aimed at: (i) the presence of methylene blue (MB), which acts as both a near-infrared (NIR) imaging agent and a leaving group; and (ii) the use of the BHA moiety as a ROS-sensitive linker. Upon exposure to ROS, the MB group dissociated from the structure to initiate a self-immolative elimination process, which resulted in the precise release of galactose attached to the benzyl alcohol arms of BHA [25].

- *Biotinylated Gal-PNPs*

Cheng et al. (2018) fabricated chitosan nanoparticles by simultaneously modifying them with galactose and biotin. To attach galactose, lactose was first reduced with sodium borohydride ($NaBH_4$) and then attached to chitosan. In the next step, biotin was attached to galactosylated chitosan as an N-hydroxysuccinimide (NHS) ester derivative. This dual targeting approach utilized the ASGPR receptor to recognize liver cells via galactose and the biotin receptor, which is overexpressed in tumor cells, to enhance tumor-specific uptake of nanoparticles [24].

- *Galactosylated Tin-doped alginate nanoparticles*

Somasundaram et al (2016) first prepared tin-doped alginate nanoparticles loaded with doxorubicin (DOX). Next, a two-step surface engineering approach was used to modify the surface of the nanoparticles. Polyethyleneimine (PEI) was first used for initial surface modification. In the second step, galactoses were covalently attached to the surface of the nanoparticles. Fourier transform infrared spectroscopy (FTIR) revealed the presence of characteristic galactose peaks, including a peak at around 1032 $cm^{-1}$ related to carbohydrate structures and a broad absorption band related to O–H/N–H stretching in the range of 2800–3500 $cm^{-1}$ [26].

- *Enzyme-responsive nanosystems*

Ma et al. (2020) designed an innovative tumor-targeting nanoimaging system in which the amphiphilic compound tetraphenylethylene (TPE) was covalently conjugated to β-D-galactose. The attachment of the galactose unit to the TPE core was accomplished via a CuAAC reaction, and all acetyl groups were subsequently removed to expose free galactose on the surface. This structural modification resulted in a nanoplatform with the ability to release drugs in response to the enzyme β-galactosidase (present in the tumor microenvironment). The TPE-Gal conjugates were self-assembled into nanovesicles. DOX was successfully loaded into these structures with a high encapsulation efficiency of 88.5% and a drug content of 15.4 wt% [30].

- *Hydroxyethyl starch-based Gal-PNPs*

In a study by Hu et al. (2017), a system of galactose-functionalized polymer nanoparticles (Gal-HES-PCL) was designed that had the capability of simultaneous imaging and therapy. In this nanoplatform, the core structure was composed of branched polycaprolactone with hydroxyethyl starch (HES-PCL); so that the hydrophobic part of PCL enabled the encapsulation of therapeutic and imaging agents, and the hydrophilic outer layer of HES increased the colloidal stability and residence time in the blood circulation. To provide specific targeting ability, galactosamine ligands were attached to the structure via an amide bond after succinylation of the middle polymer chain. In the final formulation, DOX and indocyanine green (ICG; as the imaging agent) were loaded into the nanocapsules [27].

- *Metabolic glycoengineering on cancer cells*

In a groundbreaking study by Wang et al. (2019), two glycan precursors, N-azidoacetylgalactosamine (GalAz) and N-azidoacetylmannosamine (ManAz), were fabricated to evaluate their ability in bioorthogonally tagging HCC cell surfaces. GalAz was prepared via direct azidoacetylation of D-galactosamine, and its structural integrity was confirmed using $^{1}H$-NMR, $^{13}C$-NMR, FTIR, and ESI-MS. These modifications formed a click reaction with dibenzocyclooctene (DBCO)-functionalized compounds, i.e., DBCO–Cy5 for imaging and DBCO–Dox for drug delivery [29].

***Imaging efficacy of Gal-PNPs***

- Fluorescence imaging for breast cancer

Imaging performance of Den@5F was tested in a 4T1 breast cancer xenograft model. After systemic injection, the Cy5 fluorescent signal significantly accumulated at the tumor site and persisted for up to 48 h, especially under UV irradiation. Compared with commonly modified galactose nanoparticles, Den@5F had significantly higher tumor specificity and signal intensity. In vitro fluorescence staining of tumor tissue sections confirmed the mechanistic basis for this improvement; UV irradiation induced photochemical conversion of sialic acid-rich surfaces on the tumor to galactose-decorated areas. The nanosystem was able to significantly increase the tumor-to-background signal ratio and maintain signal stability over time. Furthermore, the local increase in galactose density in tumors may enhance their immune recognition, indicating their possible theranostic utility [23].

- *Fluorescence imaging for HCC*

Imaging efficacy of Bio-GC nanoparticles was assessed in an orthotopic model of HCC developed by H22 cells in mice. Based on in vitro studies, Bio-GC nanoparticles showed significantly higher uptake in HCC cells (SMMC-7721) than control formulations containing non-targeted chitosan (CS) and single ligand nanoparticle (GC). Moreover, Bio-GC nanoparticles' uptake in normal liver cells (LO2) was also very low, which indicated their high tumor specificity. This enhanced uptake was mainly due to biotin receptor-dependent endocytosis; biotin receptor expression in HCC cells was reported to be about 39.6-fold higher than in normal liver tissue. According to in vivo imaging using the Maestro™ system at different time points after injection (2–24 h), Rhodamine B isothiocyanate (RBITC)-labeled Bio-GC nanoparticles showed the highest fluorescence intensity in the tumor area and the highest tumor-to-liver contrast ratio (C/L) at 24 h [24].

Imaging performance of Gal-micelles was evaluated in a subcutaneous model of HCC established by injecting Huh7 cells into nude mice. These nanosystems exhibited a significantly higher cellular uptake in ASGPR-positive cells, such as HepG2 and Huh7, as shown by confocal microscopy images and flow cytometry. This finding confirmed the efficiency of receptor-specific targeting due to galactose binding. At the intracellular level, Gal-micelles were associated with efficient escape from the endosomal trap and accumulation in the cytoplasm, which was mediated by the "proton sponge" effect of the PDMAEMA moiety, which disrupted the endosomal membrane. Based on in vivo imaging data, rhodamine B-labeled Gal-micelles had a strong, tumor-specific fluorescence signal up to 72 hours after injection. Compared with Glc-micelles and untargeted samples, Gal-micelles showed significantly higher accumulation in tumor tissue. These results suggest that Gal-micelles have the potential to enhance contrast and signal persistence in optical imaging of liver tumors [28].

Targeting efficiency of galactose-conjugated zwitterionic nanocarriers was investigated in a mouse model of subcutaneous HepG2 tumors. Confocal microscopy images revealed their uptake in HepG2 cells, with negligible entry into normal NIH3T3 fibroblast cells. In an in vivo pharmacokinetic study, the nanoplatform had a long circulation half-life in the blood (about 14.4

h). This effect was due to the presence of the PSBMA zwitterionic coating, which reduced their opsonization and reticuloendothelial system clearance. To evaluate the imaging performance, a BODIPY-based fluorescence probe was loaded into the nanocarrier. In vivo imaging showed a clear accumulation of fluorescence signal at the tumor site [34].

The biological function of TPE-Gal@DOX nanovesicles was investigated in the HepG2 tumor-bearing mouse model and L02 normal liver cells. Confocal laser scanning microscopy imaging showed that the nanovesicles entered HepG2 cells in a time-dependent manner; blue (TPE) and red (DOX) fluorescence signals clearly confirmed the cellular entry and intracellular trafficking pathway. DOX first accumulated in lysosomes and then translocated to the nucleus, indicating a pH-dependent release activated by β-galactosidase. In contrast, in normal L02 cells, the DOX signal was very small, indicating high specificity of targeting cancer cells. This specificity was due to the specific galactose–galectin-1 interaction as well as the enhanced EPR effect. TPE core with its emission-induced aggregation (AIE) property enabled live, label-free imaging. Based on in vivo fluorescence imaging data, there was a strong accumulation of the nanovesicles in tumor tissue. These results suggested the theranostic potential of TPE-Gal@DOX nanovesicles for the specific diagnosis and treatment of HCC [30].

- *Near-infrared fluorescence imaging for HCC*

Imaging efficacy of FDROS-7 was tested in ASGPR receptor-positive (HepG2) and negative (RAW) cells to assess its ability to target tumors. Confocal imaging results showed that the entry of FDROS-7 into HepG2 cells was time-dependent and mediated by a specific galactose–ASGPR interaction; this uptake was significantly inhibited by competition with free galactose, confirming a specific role for targeting. ROS-sensitivity of this system was tested by pretreatment of cells with N-acetyl-L-cysteine. Under these conditions, the activation of the fluorophore methylene blue was significantly suppressed, confirming its ROS-induced fluorescence ability. During NIR imaging of HepG2 tumor-bearing mice, a strong and localized signal was recorded in the tumor area within 24 hours after injection. Control treatments with saline or a non-targeted version of FDROS-5 lacked such a significant fluorescence signal, indicating the necessity of simultaneous galactose targeting and ROS response for effective imaging efficacy. In vitro organ imaging also confirmed the high accumulation of FDROS-7 in the liver and tumor tissues [25].

In vivo NIR fluorescence imaging showed that the tumor uptake of galactose-modified nanoparticles was significantly higher than that of untargeted nanoparticles and the free form of the ICG fluorescent dye. This increase in uptake, reported to be between 1.6 and 3.3-fold, was attributed to a dual targeting mechanism: nonspecific accumulation via enhanced EPR effect and active uptake via ASGPR-mediated endocytosis. In this system, ICG was encapsulated as an NIR fluorescent probe to monitor biodistribution of the nanosystem. Gal-HES-PCL nanoparticles showed maximum tumor fluorescence intensity at 24 h after injection, and this signal was maintained for up to 96 h. Quantitative analysis indicated that the signal intensity in the targeted nanoparticle group was 1.4–2.2 times higher than that of free ICG or galactose-free nanoparticles, indicating longer tumor localization and improved imaging contrast [27].

- *Metabolic labeling and imaging with GalAz for HCC*

The biological function of GalAz was evaluated in a HepG2 xenograft tumor mouse model. After intravenous injection, GalAz was able to efficiently introduce azide groups metabolically onto the surface of tumor cells, allowing for bioorthogonal conjugation with DBCO-labeled imaging probes. Compared with ManAz, GalAz induced a much higher surface azide density in a dosedependent manner; concentrations up to 50 μM resulted in a higher fluorescence signal due to DBCO–Cy5 binding. In vivo fluorescence imaging showed that GalAz-treated mice had significantly stronger tumor-specific signals than ManAz or PBS groups. Confocal microscopy also confirmed the increased surface azide expression and efficient probe binding at the tumor site. Radiolabeled biodistribution analysis showed that $^{14}C$-GalAz accumulated in tumor tissue by 195% more than $^{14}C$-ManAz (five days after injection). The high tumor-to-liver signal ratio suggested that GalAz was more efficiently incorporated into glycoprotein biosynthesis pathways [29].

- *Nuclear imaging and photothermal imaging for HCC*

Flow cytometry analysis showed that tin-doped, galactose-decorated alginate nanoparticles had a significantly higher uptake in HepG2. These nanoplatforms exhibited a nearly 91% uptake within 30 min, which was significantly higher than that for the galactose-free nanoparticles (with 81%). Technetium-99m ($^{99m}Tc$)-labelled GAD NPs were synthesized with a radiolabeling efficiency of 80%. Gamma scintigraphy and radiographic imaging in healthy male Sprague-Dawley rats showed that the major accumulation of nanoparticles occurred in the liver, peaking at 40 min after injection. Area under the curve (AUC) analysis also confirmed the effective ASGPR-targeting of the liver. Targeting efficacy of this platform was also tested in the N1S1 liver tumor model. After injection of nanoparticles and irradiation with near-infrared light, selective photothermal activation was observed in tumor tissues. Infrared thermographic imaging showed that the temperature of the tumor tissue increased to about 62°C, while the temperature of the surrounding healthy tissue was about 42°C [26].

- *PET/CT for bladder cancer*

The imaging effect of the galactodendrite nanoprobe was evaluated in an orthotopic bladder tumor model derived from human transitional cell carcinoma UMUC3 cells in mice. Due to the overexpression of galectin-1 in tumor cells, this nanoprobe showed selective and significant accumulation in tumor tissue. In contrast, healthy bladder tissue showed very little uptake, confirming the specificity of targeting and the reduction of unwanted background signals. The performance of this nanoprobe was evaluated using PET/CT imaging. Quantitative analysis of the images showed that the $SUV_{mean}$ value was significantly higher in tumor-bearing mice ($43.5 \pm 4.2$) compared to tumor-free mice ($2.0 \pm 0.4$). In particular, this galactose nanoprobe showed better performance than the conventional $^{18}F$-FDG tracer ($SUV_{mean} = 10.5 \pm 2.3$) and provided a higher tumor-to-background contrast ratio [32].

- *Fluorescence imaging for glioblastoma*

The biological function of glycosylated dendrimers was investigated in a mouse model of glioblastoma (GL261 cells) with a focus on the interaction with tumor cells and the tumor microenvironment. Fluorescence imaging of mouse brains 24 hours after intravenous injection showed that D-GLU accumulated most in the tumor ($15.0 \pm 4.7$ μg/g), which was approximately 8-fold higher than that of unmodified D-OH ($1.9 \pm 0.3$ μg/g, $p < 0.001$). D-GAL also showed significant accumulation in the tumor, with a tumor-to-contrast hemisphere ratio of 7.1, which was higher than D-OH (3.4) and D-MAN (4.0), but lower than D-GLU (18.8). In particular, D-GAL was mainly accumulated in the extracellular matrix (ECM), in contrast to D-GLU and D-MAN, which were more co-localized with tumor-associated macrophages (TAMs) and microglia. This distribution was due to the specific interaction between D-GAL and galectins. Based on an in vitro binding assay, D-GAL had a higher affinity for the membrane of GL261 cells than D-OH (p=0.027), which was significantly reduced after pretreatment with α-lactose (p=0.0095). This confirmed the role of galectin-mediated targeting in this system. In this study, fluorescence imaging with Cy5 labeling showed that D-GAL had a significantly higher tumor-to-background contrast ratio, which strengthens its potential application in molecular imaging of tumors with high galectin expression [33].

**Targeted imaging of non-solid tumors**

Only one study was found for non-solid tumor models. Compared with solid tumor imaging, this study demonstrated that Gal-PNPs were able similarly to achieve high receptor-mediated specificity and signal intensity, suggesting potential applicability in liquid biopsy and circulating tumor cell detection. This new nanoparticle system was developed for sensitive detection of circulating tumor cells from hepatocellular carcinoma (HCC-CTCs) in blood samples. This nanoplatform was employed as a reduced graphene oxide (rGO) film with an anti-EpCAM antibody coating, which was conjugated with galactose-rhodamine-decorated polyacrylamide nanoparticles (Gal-Rh-PAA NPs). The system is designed to simultaneously utilize the EpCAM receptor for tumor cell capture and the ASGPR receptor for targeted internalization and fluorescence signal recovery. Gal-Rh-PAA nanoparticles of 10–20 nm quenched rhodamine fluorescence on adsorption onto the graphene film. Upon introduction of these nanoparticles into ASGPR-expressing CTC cells, the fluorescence was recovered, and one-step imaging was enabled. Spectral analysis revealed rhodamine excitation and emission peaks of 520 and 555 nm. Moreover, zeta potential changed from -20 mV in unstained nanoparticles to -5 mV after rhodamine binding. Compared to control systems, the platform was more efficient in cell uptake and optical signal recovery. This platform was able to identify cells with good accuracy even at low density (5 cells per ml). HepG2 cells produced more than 7 times the fluorescence of non-hepatic cancerous cell lines (such as HeLa and MCF-7), demonstrating the high specificity of the system. In addition to single cells, the technology also identified CTC clusters with higher metastasis potential. In HCC patient blood samples (stages III-IVB), the number of CTCs detected was proportional to the stage of disease, and no CTCs were seen in normal volunteers or ICC patients. Immunofluorescent staining with CK8+/CD45-/DAPI+ markers also confirmed the actual presence of CTCs [31].

**Biosafety profile of GAL-PNPs**

The Den@5F nanoprobe did not show any observable histological abnormalities in major organs, such as the heart, liver, spleen, lung, and kidney [23]. Also, glycosylated dendrimers such as D-GAL, D-MAN, and D-OH were associated with rapid systemic clearance, with plasma levels reaching less than 1% of the injected dose within 24 h. Renal excretion was the predominant route, and there was negligible uptake for Kupffer cells (immunological safety) [33]. Moreover, intravesically injected galactodendrite nanoprobes showed an efficient clearance through excretory and metabolic organs. However, little signal was observed in bone, which was attributed to the byproducts of its degradation [32]. Therefore, dendrimer-based Gal-PNPs may be well-tolerated for systemic injection in molecular imaging.

In addition, Bio-GC nanoparticles showed no observable toxicity in normal liver tissue and significantly increased survival in tumor-bearing mice [24]. In addition, extracorporeal organ imaging showed that FDROS-7 had negligible off-target accumulation in vital organs, including the heart, kidneys, lungs, and spleen. Furthermore, the cytotoxicity of FDROS-7 in cells lacking the ASGPR receptor, such as RAW macrophages, was significantly lower, emphasizing its biotargeting specificity and low likelihood of unwanted side effects [25]. Moreover, Gal-micelles were accumulated mainly in liver and tumor tissue during the first 24 hours after injection and then excreted via the kidneys [28].

The Gal-HES-PCL nanosystem did not show any signs of organ toxicity, and its hydrophilic HES coating appeared to reduce immunogenicity and increase systemic circulation time [27]. Moreover, tin-containing alginate nanoparticles showed no off-target distribution [26]. Furthermore, TPE-Gal@DOX nanovesicles induced less than 5% hemolytic activity up to a concentration of 1000 μg/mL. No significant weight loss or signs of systemic toxicity were observed in the treated animals during the study period. Based on biodistribution analysis, their accumulation in the heart, spleen, lung, and kidney was significantly lower than that of free DOX [30]. Regarding galactose-functionalized zwitterionic polymers, histopathological evaluation did not reveal any signs of tissue damage or inflammation in the liver, spleen, or kidney after systemic administration [34]. Lastly, the GalAz-based glycometabolic engineering approach did not show any obvious systemic toxicity. Hepatic accumulation remained within safe limits [29].

**Risk of Bias Assessment**

The methodological quality of the included studies was assessed in ten domains (D1–D10) using the SYRCLE risk of bias tool (Figure 2) [42]. Overall, the studies showed a low to moderate risk of bias, with most domains assessed as low risk and a smaller proportion as unclear. The summary of the overall risk of bias (Figure 2B) showed that approximately 70–80% of the assessments were assessed as low risk, with no domains classified as high or critical risk [23-34].

In particular, random sequence generation (D1) and baseline characteristics (D2) were largely assessed as low risk. This indicated adequate experimental randomization and the comparability of animal models at baseline. However, allocation concealment (D3) and maintenance of randomization (D4) were often reported as unclear due to insufficient methodological details. Similarly, some uncertainty remained for blinding of investigators (D5) and outcome assessment (D7), which may introduce observer bias.

The assessment domains of attribution bias (D8), reporting bias (D9), and other sources of bias (D10) were mostly assessed as low risk. These findings suggest that the available evidence base is methodologically robust and that the low risk of bias supports the validity of the biosafety and efficacy results reported for Gal-PNPs.

## DISCUSSION

In the last decade, Gal-PNPs have emerged as promising nanoplatforms for precision cancer imaging and theranostics. By exploiting the overexpression of ASGPR and galectins in the tumor microenvironment, Gal-PNPs facilitate receptor-mediated uptake and achieve enhanced signal-to-background contrast. Diverse conjugation strategies, including click chemistry, amide coupling, ring-opening reactions, and glycan engineering, have enabled the design of structurally and functionally tailored Gal-PNPs. Numerous preclinical studies have validated their efficacy across multiple molecular imaging modalities, including fluorescence, near-infrared, positron emission tomography/computed tomography, nuclear scintigraphy, and photothermal imaging.

Hepatocellular carcinoma has emerged as the most widely used tumor model, due to the high expression levels of ASGPR on liver cells [24-28, 30, 31, 34]. Several studies have shown that Gal-PNPs selectively accumulate in ASGPR-positive tumors, such as HepG2 and Huh7, while their uptake in normal liver cells (such as LO2 cells) or ASGPR-deficient models is minimal. The high tumor uptake of these nanoparticles provides strong arguments for the application of

galactose-based nanosystems in liver tumor imaging [24-28, 30, 31, 34]. Notably, the use of dual targeting approaches, for example, biotin-containing galactosylated nanoparticles, has been able to significantly increase the specificity and signal intensity of this platform [24].
In addition, Gal-PNPs have also shown strong potential in non-hepatic tumors, such as CTCs, breast, bladder, and glioblastoma [23, 31-33]. For example, in the 4T1 breast tumor model, UV-induced sialic acid conversion to galactose increased nanoprobe binding [23]. In glioblastoma, galactosylated dendrimers exhibited stronger extracellular matrix accumulation due to galectin–galactose affinity [33], while PET/CT-based bladder imaging showed superior contrast ratios driven by galectin-1 overexpression [32].
Among different molecular imaging methods, fluorescence imaging remains the most commonly used technique for Gal-PNPs. The reason is possibly the availability of a wide range of fluorescent dyes, such as Cy5, BODIPY, RBITC, and TPE, which allow for precise and sensitive tracking of nanocarriers in the biological environment [23-25, 27, 28, 30, 31, 33, 34]. Among the new platforms developed in this field, the TPE-Gal@DOX structure can be mentioned; by utilizing the phenomenon of dual emission, this system allows us to combine targeted drug delivery with high-resolution imaging in an integrated system [30].
Another important development is the application of near-infrared fluorescence imaging systems using nanomaterials such as FDROS-7 and Gal-HES-PCL [25, 27]. These systems help achieve greater penetration of imaging agents into deep tissues [25, 27]. In particular, FDROS-7 is specifically activated in the tumor microenvironment because it is designed to respond to high levels of ROS in cancer cells. This unique property reduces non-specific signals in healthy tissues and increases imaging accuracy [25]. Also, the simultaneous combination of nuclear imaging and photothermal imaging using tin- and galactose-doped alginate nanoparticles is another example of dual systems that not only enable precise imaging but also provide targeted thermal therapy. This intelligent approach opens new horizons in imaging-based therapeutic interventions [26].
Importantly, nuclear imaging platforms, notably PET/CT and gamma scintigraphy, have expanded the translational potential of Gal-PNPs. In comparative preclinical analyses, radiolabeled Gal-PNPs achieved higher tumor-to-liver ratios and longer circulation times than the standard $^{18}$F-FDG tracer, demonstrating promise for quantitative, whole-body molecular imaging [32]. Additionally, tin–galactose alginate nanoparticles combined nuclear imaging with photothermal therapeutic capabilities, showcasing the potential of dual-function theranostic systems [26].
From an industrial manufacturing perspective, dendrimer-based systems are economically more expensive. This is mainly due to the use of high-purity monomers and the need for multi-step synthesis and chromatographic purification procedures [43]. Copolymer micelles, nanoparticles based on hydroxyethyl starch, and systems conjugated with chitosan are cost-effective alternatives. Such systems allow mass production at reduced cost due to the easy availability of commercial polymers and the requirement of simpler post-synthetic modification. Alginate and starch derivatives are also prepared under relatively mild conditions and are thus especially suitable for scaling up to GMP-compliant manufacturing facilities. Yet another highly specific, safe, and low-cost strategy is the use of biotin-galactose bidirectional targeting systems [23-34].
From a physicochemical perspective, two of the most critical parameters were particle size and zeta potential. They have a direct impact on colloidal stability, biodistribution pattern, and permeability across tumor tissue [44, 45]. According to the results of different studies, the size of the nanoparticles varied from around 4.5 nm to more than 150 nm [27, 28, 33]. Smaller nanoparticles, such as D-GAL, had a greater probability of entering the tumor extracellular matrix due to their size being close to the molecular dimension, while larger nanoparticles, such as Gal-

HES-PCL, had a greater possibility of aggregating in the tumor through the EPR effect and the ASGPR receptor [27, 33].

Physicochemically, Gal-PNPs exhibit particle sizes ranging from 4.5 nm to >150 nm and zeta potentials between −26 mV and +39.2 mV, parameters that strongly influence stability, permeability, and biodistribution [24, 26, 27, 33]. Nanoparticles with a positive surface charge have a higher tendency to interact with the negatively charged cell membrane and therefore can play an important role in cellular uptake [24, 46-48]. However, nanoparticles with a negative zeta potential also have higher colloidal stability, which increases the circulation time in the blood and reduces unwanted uptake by the reticuloendothelial system [31, 49, 50]. In contrast, nanoparticles with a neutral surface charge were able to attain high targeting efficiency independent of high surface charge by activating other active mechanisms, such as photocrosslinking and tumor surface receptors [33, 51].

Dendrimer-based platforms, despite having precise structural order and high functional ability, are usually associated with high cytotoxicity. This is mainly due to the presence of positively charged terminal amino groups in their structure, which can disrupt the cell membrane. Therefore, targeted surface design, such as PEG-binding or attachment of sugars or negatively-charged functional groups (such as OH and COOH) to the dendrimer surface, is among strategies to reduce the toxicity of these systems. Hopefully, their surface modification with PEGylation or conjugation with sugars and negatively-charged functional groups (such as OH and COOH) has improved the biosafety of these dendrimers [31, 49, 50]. Also, tumor-responsive systems, by introducing new chemical groups, such as arylamines or self-immolative linkers, may generate several degradation byproducts whose safety requires more careful evaluation [25]. On the other hand, metal-doped systems and nanoparticles labeled with radioisotopes require thorough toxicological profiling [26]. From a safety perspective, most studies reported no significant histological abnormalities in major organs [23-34]. Nevertheless, the present systematic review also acknowledges certain methodological limitations. Risk of bias assessment (Figure 2) showed that approximately 70–80% of the studies were at low risk of bias, particularly for randomized sequence generation, outcome assessment, and reporting. However, allocation concealment and investigator blinding were often unclear due to incomplete reporting [23-34]. These uncertainties may influence the precision of biosafety and efficacy estimates. Despite this, the predominance of low bias across domains strengthens confidence in the observed safety and imaging reliability of Gal-PNPs [23-34].

From a translational perspective, dendrimer-based systems offer superior functional versatility but remain cost-intensive, requiring multi-step synthesis and chromatographic purification [43]. In contrast, copolymer micelles, hydroxyethyl starch conjugates, and chitosan-based systems provide cost-effective, scalable alternatives suitable for GMP-compliant manufacturing. Finally, future studies should aim to improve methodological transparency, particularly in randomization, blinding, and quantitative nuclear imaging metrics, to meet standards and facilitate clinical translation of these preclinical findings [42, 52, 53]. Overall, the cumulative evidence supports Gal-PNPs as highly promising [32], biocompatible nanocarriers for targeted PET/CT and multimodal imaging applications in cancer theranostics.

## CONCLUSION

This systematic review discusses different chemical strategies applied for conjugating galactose to various polymeric nanoparticles (from dendrimers and micelles to natural polymers, such as chitosan, hydroxyethyl starch, and alginates). These methods vary from click chemistry, amide bond formation, covalent ring-opening, and glycoengineering. These platforms have been promising in the molecular imaging of both hepatic and non-hepatic tumors. These systems have been successful in improving the imaging efficacy of several cancer imaging modalities, including fluorescence imaging, near-infrared imaging, positron emission tomography/computed tomography, nuclear imaging, and photothermal imaging. The results demonstrate their multimodality and therapeutic-diagnostic (theranostic) potential. This safe approach exhibited high tumor selectivity, signal persistence and strength, a high signal-to-noise ratio, and a high tumor-to-background contrast. Among them, dendrimer-based platforms (such as Den@5F) and stimuli-responsive systems (such as FDROS-7, TPE-Gal, Bio-GC, and GalAz) have shown superior imaging performance, which is due to features such as multiple galactose linkages, dual targeting capability, and selective activation in tumor tissue.

This review also highlights certain limitations. Most studies have focused on liver models, with little research in non-hepatic tumors, and several preclinical reports lacked complete blinding or allocation concealment, as reflected in the risk of bias assessment. Furthermore, quantitative data on long-term biodistribution, radiolabeling stability, and in vivo dosimetry remain limited, particularly for nuclear imaging modalities. Therefore, future studies should focus on extending the evaluation of Gal-PNP to non-hepatic cancers and validating its performance in nuclear and combined imaging techniques such as PET/CT and SPECT. Integrating these findings into multimodality imaging systems may ultimately increase diagnostic accuracy, depth of penetration, and clinical translation in cancer theranostics.

**Abbreviation list**

PNPs, polymer nanoparticles; MPS, mononuclear phagocyte system; ABC, accelerated blood clearance; Gal-PNPs, galactose-functionalized polymeric nanoparticles; ASGPR, the asialoglycoprotein receptor; HCC, hepatocellular carcinoma; MRI, magnetic resonance imaging; PET, positron emission tomography; CT, computed tomography; CuAAC, copper-catalyzed alkyne-azide click reaction; Cyt5, cyanine 5; PBA, Phenylboronic acid; mNB, photocrosslinking group of 4-(4-(hydroxymethyl)-2-methoxy-5-nitrophenoxy)butanoate; EDC/NHS, N-(3-dimethylaminopropyl)-N'-ethylcarbodiimide hydrochloride/N-hydroxysuccinimide; Bio-GC, galactosylated chitosan nanoparticles; 5-FU, 5-fluorouracil; NHS, N-hydroxysuccinimide; RBITC, rhodamine B isothiocyanate; ROS, reactive oxygen species; MB, methylene blue; NIR, near-infrared; CLB, chlorambucil; DOX, doxorubicin; PEI, polyethyleneimine; AD NPs, tin-doped alginate nanoparticles; AUC, area under the curve; ICG, indocyanine green; Gal, Galactose; DEE, drug encapsulation efficiency; DLC, drug loading capacity; GalAz, N-azidoacetylgalactosamine; ManAz, N-azidoacetylmannosamine; DBCO, dibenzocyclooctyne; TPE, tetraphenylethene; AIE, aggregation-induced fluorescence; CLSM, Confocal laser scanning microscopy; rGO, reduced graphene oxide; Gal-Rh-PAA NPs, galactose-rhodamine-decorated polyacrylamide nanoparticles; TAMs, tumor-associated macrophages; RES, the reticuloendothelial system.

## REFERENCES


1. Bray F, Laversanne M, Sung H, Ferlay J, Siegel RL, Soerjomataram I, Jemal A. Global cancer statistics 2022: GLOBOCAN estimates of incidence and mortality worldwide for 36 cancers in 185 countries. CA Cancer J Clin. 2024 May-Jun;74(3):229-63.
2. Crosby D, Bhatia S, Brindle KM, Coussens LM, Dive C, Emberton M, Esener S, Fitzgerald RC, Gambhir SS, Kuhn P, Rebbeck TR, Balasubramanian S. Early detection of cancer. Science. 2022 Mar 18;375(6586):eaay9040.
3. Pulumati A, Pulumati A, Dwarakanath BS, Verma A, Papineni RVL. Technological advancements in cancer diagnostics: improvements and limitations. Cancer Rep (Hoboken). 2023 Feb;6(2):e1764.
4. Tantray J, Patel A, Parveen H, Prajapati B, Prajapati J. Nanotechnology-based biomedical devices in the cancer diagnostics and therapy. Med Oncol. 2025 Jan 20;42(2):50.
5. Yin C, Hu P, Qin L, Wang Z, Zhao H. The current status and future directions on nanoparticles for tumor molecular imaging. Int J Nanomedicine. 2024 Sep 14;19:9549-74.
6. Al-Thani AN, Jan AG, Abbas M, Geetha M, Sadasivuni KK. Nanoparticles in cancer theragnostic and drug delivery: A comprehensive review. Life Sci. 2024 Sep 1;352:122899.
7. Umadevi K, Sundeep D, Vighnesh AR, Misra A, Krishna AG. Current trends and advances in nanoplatforms-based imaging for cancer diagnosis. Indian J Microbiol. 2025 Mar;65(1):137-76.
8. Gu X, Minko T. Targeted nanoparticle-based diagnostic and treatment options for pancreatic cancer. Cancers (Basel). 2024 Apr 20;16(8):1589.
9. Habeeb M, Vengateswaran HT, Tripathi AK, Kumbhar ST, You HW, Hariyadi. Enhancing biomedical imaging: the role of nanoparticle-based contrast agents. Biomed Microdevices. 2024 Oct 23;26(4):42.
10. Jena BR, Dash R, Mishra H. Polymeric nanoparticles used in biosensors. InMaterials and Components of Biosensors in Healthcare. Academic Press; 2025. p. 71-90.
11. Haidar LL, Bilek M, Akhavan B. Surface Bio-engineered polymeric nanoparticles. Small. 2024 May;20(21):e2310876.
12. Shen Q, Song G, Lin H, Bai H, Huang Y, Lv F, Wang S. Sensing, imaging, and therapeutic strategies endowing by conjugate polymers for precision medicine. Adv Mater. 2024 May;36(19):e2310032.
13. Wang J, Lu B, Yin G, Liu L, Yang P, Huang N, Zhao A. Design and fabrication of environmentally responsive nanoparticles for the diagnosis and treatment of atherosclerosis. ACS Biomater Sci Eng. 2024 Mar 11;10(3):1190-206.
14. Gaddimath S, Payamalle S, Channabasavana Hundi Puttaningaiah KP, Hur J. Recent advances in pH and redox responsive polymer nanocomposites for cancer therapy. J Compos Sci. 2024;8(1):28.
15. Shi Y, Yu Q, Tan L, Wang Q, Zhu WH. Tumor microenvironment-responsive polymer delivery platforms for cancer therapy. Angew Chem Int Ed Engl. 2025 Jun 24;64(26):e202503776.
16. Hu T, Shen C, Wang X, Wu F, He Z. Tumor microenvironment-sensitive polymeric nanoparticles for synergetic chemo-photo therapy. Chin Chem Lett. 2024 Nov 1;35(11):109562.
17. Tao Q, Wen Y, Liang W, Wang L, Guo R, Ding M, Luo M, Yan J, Gong F, Cao C, Li L. Development of ratiometric DNA biosensors with improved accuracy, precision, and signal-to-noise ratio. Adv Sens Energy Mat. 2024 Sep 1;3(3):100106.
18. Mills JA, Liu F, Jarrett TR, Fletcher NL, Thurecht KJ. Nanoparticle based medicines: approaches for evading and manipulating the mononuclear phagocyte system and potential for clinical translation. Biomater Sci. 2022 Jun 14;10(12):3029-53.
19. Abu Lila AS, Kiwada H, Ishida T. The accelerated blood clearance (ABC) phenomenon: clinical challenge and approaches to manage. J Control Release. 2013 Nov 28;172(1):38-47.
20. Zielińska A, Carreiró F, Oliveira AM, Neves A, Pires B, Venkatesh DN, Durazzo A, Lucarini M, Eder P, Silva AM, Santini A, Souto EB. Polymeric nanoparticles: production, characterization, toxicology and ecotoxicology. Molecules. 2020 Aug 15;25(16):3731.
21. Li J, Chang X, Chen X, Gu Z, Zhao F, Chai Z, Zhao Y. Toxicity of inorganic nanomaterials in biomedical imaging. Biotechnol Adv. 2014 Jul-Aug;32(4):727-43.
22. Wang J, Wang H, Zou F, Gu J, Deng S, Cao Y, Cai K. The role of inorganic nanomaterials in overcoming challenges in colorectal cancer diagnosis and therapy. Pharmaceutics. 2025 Mar 25;17(4):409.
23. Yang Y, Li Y, Wang C, Wang Y, Ren Y, Wu J, Ju H, Chen Y. Ultra-galactocation to sialic acid on tumor cells with a penta-functional dendritic probe for enhanced immune-killing. Angew Chem Int Ed Engl. 2024 May 13;63(20):e202319849.
24. Cheng M, Ma D, Zhi K, Liu B, Zhu W. Synthesis of biotin-modified galactosylated chitosan nanoparticles and their characteristics in vitro and in vivo. Cell Physiol Biochem. 2018;50(2):569-84.

25. Liu F, Liu L, Wei P, Yi T. A reactive oxygen species-triggerable theranostic prodrug system. J Control Release. 2024 Dec;376:961-71.
26. Somasundaram VH, Pillai R, Malarvizhi G, Ashokan A, Gowd S, Peethambaran R, Palaniswamy S, Unni A, Nair S, Koyakutty M. Biodegradable radiofrequency responsive nanoparticles for augmented thermal ablation combined with triggered drug release in liver tumors. ACS Biomater Sci Eng. 2016 May 9;2(5):768-79.
27. Hu H, Xiao C, Wu H, Li Y, Zhou Q, Tang Y, Yu C, Yang X, Li Z. Nanocolloidosomes with selective drug release for active tumor-targeted imaging-guided photothermal/chemo combination therapy. ACS Appl Mater Interfaces. 2017 Dec 6;9(48):42225-38.
28. Ye Z, Wu WR, Qin YF, Hu J, Liu C, Seeberger PH, Yin J. An integrated therapeutic delivery system for enhanced treatment of hepatocellular carcinoma. Adv Funct Mater. 2018;28(18):1706600.
29. Wang H, Liu Y, Xu M, Cheng J. Azido-galactose outperforms azido-mannose for metabolic labeling and targeting of hepatocellular carcinoma. Biomater Sci. 2019 Oct 1;7(10):4166-73.
30. Ma W, Bi J, Wu H, Zhang G. An amphiphilic micromolecule self-assembles into vesicles for visualized and targeted drug delivery. ACS Med Chem Lett. 2020 Jul 20;11(8):1562-6.
31. Wu C, Li P, Fan N, Han J, Zhang W, Zhang W, Tang B. A dual-targeting functionalized graphene film for rapid and highly sensitive fluorescence imaging detection of hepatocellular carcinoma circulating tumor cells. ACS Appl Mater Interfaces. 2019 Dec 4;11(48):44999-5006.
32. Pereira PMR, Roberts S, Figueira F, Tomé JPC, Reiner T, Lewis JS. PET/CT imaging with an 18F-labeled galactodendritic unit in a galectin-1-overexpressing orthotopic bladder cancer model. J Nucl Med. 2020 Sep;61(9):1369-75.
33. Sharma R, Liaw K, Sharma A, Jimenez A, Chang M, Salazar S, Amlani I, Kannan S, Kannan RM. Glycosylation of PAMAM dendrimers significantly improves tumor macrophage targeting and specificity in glioblastoma. J Control Release. 2021 Sep 10;337:179-92.
34. An J, Guo Q, Zhang P, Sinclair A, Zhao Y, Zhang X, Wu K, Sun F, Hung HC, Li C, Jiang S. Hierarchical design of a polymeric nanovehicle for efficient tumor regression and imaging. Nanoscale. 2016 Apr 28;8(17):9318-27.
35. Zhang N, Liu Q, Wang D, Wang X, Pan Z, Han B, He G. Multifaceted roles of galectins: from carbohydrate binding to targeted cancer therapy. Biomark Res. 2025 Mar 25;13(1):49.
36. D'Souza AA, Devarajan PV. Asialoglycoprotein receptor mediated hepatocyte targeting - strategies and applications. J Control Release. 2015 Apr 10;203:126-39.
37. Rabinovich GA. Galectin-1 as a potential cancer target. Br J Cancer. 2005 Apr 11;92(7):1188-92.
38. Zou Y, Song Y, Yang W, Meng F, Liu H, Zhong Z. Galactose-installed photo-crosslinked pH-sensitive degradable micelles for active targeting chemotherapy of hepatocellular carcinoma in mice. J Control Release. 2014 Nov 10;193:154-61.
39. Lou S, Gao S, Wang W, Zhang M, Zhang J, Wang C, Li C, Kong D, Zhao Q. Galactose-functionalized multi-responsive nanogels for hepatoma-targeted drug delivery. Nanoscale. 2015 Feb 21;7(7):3137-46.
40. Peng YY, Diaz-Dussan D, Kumar P, Narain R. Tumor microenvironment-regulated redox responsive cationic galactose-based hyperbranched polymers for siRNA delivery. Bioconjug Chem. 2019 Feb 20;30(2):405-12.
41. Page MJ, McKenzie JE, Bossuyt PM, Boutron I, Hoffmann TC, Mulrow CD, Shamseer L, Tetzlaff JM, Akl EA, Brennan SE, Chou R, Glanville J, Grimshaw JM, Hróbjartsson A, Lalu MM, Li T, Loder EW, Mayo-Wilson E, McDonald S, McGuinness LA, Stewart LA, Thomas J, Tricco AC, Welch VA, Whiting P, Moher D. The PRISMA 2020 statement: an updated guideline for reporting systematic reviews. BMJ. 2021 Mar 29;372:n71.
42. Hooijmans CR, Rovers MM, de Vries RB, Leenaars M, Ritskes-Hoitinga M, Langendam MW. SYRCLE's risk of bias tool for animal studies. BMC Med Res Methodol. 2014 Mar 26;14:43.
43. Walter MV, Malkoch M. Simplifying the synthesis of dendrimers: accelerated approaches. Chem Soc Rev. 2012 Jul 7;41(13):4593-609.
44. Ernsting MJ, Murakami M, Roy A, Li SD. Factors controlling the pharmacokinetics, biodistribution and intratumoral penetration of nanoparticles. J Control Release. 2013 Dec 28;172(3):782-94.
45. Duan X, Li Y. Physicochemical characteristics of nanoparticles affect circulation, biodistribution, cellular internalization, and trafficking. Small. 2013 May 27;9(9-10):1521-32.
46. Zadeh Mehrizi T. Assessment of the effect of polymeric nanoparticles on storage and stability of blood products (red blood cells, plasma, and platelet). Polym Bull. 2023 Mar;80(3):2263-98.

47. Mehrizi TZ, Ardestani MS. The introduction of dendrimers as a new approach to improve the performance and quality of various blood products (platelets, plasma and erythrocytes): a 2010-2022 review study. Curr Nanosci. 2023 Jan 1;19(1):103-22.
48. Zadeh Mehrizi T, Shafiee Ardestani M, Rezayat SM, Javanmard A. A review study of the use of modified chitosan as a new approach to increase the preservation of blood products (erythrocytes, platelets, and plasma products): 2010-2022. Nanomed J. 2023 Jan 1;10(1):16-32.
49. Zadeh Mehrizi T, Shafiee Ardestani M, Mirzaei M, Javanmard A. A review study on the application of polymeric-based nanoparticles as a novel approach for enhancing the stability of albumins. Nanomed J. 2022 Oct 1;9(4):261-72.
50. Mehrizi TZ, Mirzaei M, Ardestani MS. Pegylation, a successful strategy to address the storage and instability problems of blood products: review 2011-2021. Curr Pharm Biotechnol. 2024;25(3):247-67.
51. Mehrizi TZ, Ardestani MS, Kafiabad SA. A review study of the influences of dendrimer nanoparticles on stored platelet in order to treat patients (2001-2020). Curr Nanosci. 2022 May 1;18(3):304-18.
52. Korde A, Mikolajczak R, Kolenc P, Bouziotis P, Westin H, Lauritzen M, Koole M, Herth MM, Bardiès M, Martins AF, Paulo A, Lyashchenko SK, Todde S, Nag S, Lamprou E, Abrunhosa A, Giammarile F, Decristoforo C. Practical considerations for navigating the regulatory landscape of non-clinical studies for clinical translation of radiopharmaceuticals. EJNMMI Radiopharm Chem. 2022 Jul 19;7(1):18.
53. McDougald W, Vanhove C, Lehnert A, Lewellen B, Wright J, Mingarelli M, Corral CA, Schneider JE, Plein S, Newby DE, Welch A, Miyaoka R, Vandenberghe S, Tavares AAS. Standardization of preclinical PET/CT imaging to improve quantitative accuracy, precision, and reproducibility: a multicenter study. J Nucl Med. 2020 Mar;61(3):461-8.

**Table 1.** Search strategy

| Database | Search Query |
|---|---|
| **PubMed (n= 36)** | (((imaging[Title/Abstract]) AND (galactose[Title/Abstract])) AND (nanoparticle[Title/Abstract])) AND (cancer[Title/Abstract]) |
| | ((("dendrites"[MeSH Terms] OR "dendrites"[All Fields] OR "dendrite"[All Fields] OR "dendritic"[All Fields] OR "dendritically"[All Fields]) AND "galactose"[Title/Abstract]) OR "hyperbranched glycopolymers"[Title/Abstract]) AND ("Neoplasms"[Title/Abstract] OR "Cancer"[Title/Abstract] OR "Tumors"[Title/Abstract] OR "Neoplasia"[Title/Abstract] OR "Malignancy"[Title/Abstract]) AND ("molecular imaging"[Title/Abstract] OR "diagnostic imaging"[Title/Abstract] OR "Imaging"[Title/Abstract]) |
| | ("Dendrimers"[Title/Abstract] OR "dendritic compounds"[Title/Abstract] OR "dendritic polymers"[Title/Abstract] OR "Dendrons"[Title/Abstract]) AND ("Galactose"[Title/Abstract] OR "Galactopyranose"[Title/Abstract] OR "Galactopyranoside"[Title/Abstract] OR "Galactosylated"[Title/Abstract]) AND ("Neoplasms"[Title/Abstract] OR "Cancer"[Title/Abstract] OR "Tumors"[Title/Abstract] OR "Neoplasia"[Title/Abstract] OR "Malignancy"[Title/Abstract]) |
| **Scopus (n= 68)** | ( TITLE-ABS-KEY ( IMAGING ) AND TITLE-ABS-KEY ( GALACTOSE ) AND TITLE-ABS-KEY ( NANOPARTICLES ) AND TITLE-ABS-KEY ( CANCER ) ) |
| **Web of Science (n=57)** | imaging (Topic) and galactose (Topic) and nanoparticle (Topic) and cancer (Topic) |

**Table 2.** Galactose-conjugated polymeric nanoparticles targeting ASGPR in hepatic tumors

| References | Model | Target | NP type | NP characteristic | Gal conjugation method | Imaging agent | Tumor uptake | Imaging efficacy | Safety |
|---|---|---|---|---|---|---|---|---|---|
| **24** | Orthotopic H22 liver cancer | ASGPR + Biotin receptor | Bio-GC NPs (Chitosan-based) | 81.1 nm; +39.2 mV; 8.98% loading; sustained release | Lactose reduction with $NaBH_4$, then biotinylation | Rhodamine B | High in SMMC-7721 (tumor cells); minimal in LO2 (normal cells) | Highest Cancer/Liver fluorescence ratio | Prolonged survival in mice |
| **25** | HepG2 tumor xenograft mice | ASGPR | FDROS-7 | ROS-responsive (200 s); High solubility | Covalent bonding via benzyl alcohols on the BHA core | Methylene blue | Highly selective uptake | Strong real-time fluorescence; cancer/liver ratio ↑ (within 24 h) | Low toxicity in RAW cells (normal cells) |
| **27** | H22 tumor-bearing mice | ASGPR | Gal-HES-PCL NCs (DOX/ICG) | ~140 nm, dandelion-like | Galactosamine conjugated to succinylated HES-PCL via amide bond | Indocyanine green | 1.6–3.3× higher uptake | Signal retention up to 96 h; High-contrast NIR imaging | No adverse effects |
| **28** | Huh7 tumor in nude mice | ASGPR | PDMAEMA–PGMA micelles | pH-sensitive; Spherical; 153.8 nm; PDI 0.24; DLC: 12.6%; DEE: 58% | CuAAC click reaction with propargyl-α-D-galactopyranoside | Rhodamine B | High in $ASGPR^+$ tumors at 6–24 h | High fluorescence intensity in $ASGPR^+$ cells and tumors | No weight loss |
| **31** | Blood samples with HCC-CTCs from human patients | ASGPR + EpCAM | Gal-Rh-PAA on rGO film | 10–20 nm; −5 mV (with Rh), −20 mV (without); Max absorb/emission: 520/555 nm | Co-polymerization using 2-propenyl-α-D-galactopyranoside into the polymer backbone | Rhodamine B | 7× stronger fluorescence in HepG2 | Detects 5 CTCs/mL | High biocompatibility |
| **34** | HepG2 tumor xenograft mice | ASGPR | Zwitterionic PSBMA/PGEA-b-PDMDEA | Spherical; ~90 nm (TEM), 100–160 nm (DLS), PDI 0.11, –7.2 mV; acid-labile; stable in serum; $t_{1/2} \approx$ 14.4 h; Lysosomal pH-triggered release | Polymerization of galactose-based PGEA block into an amphiphilic copolymer | BODIPY | Highly selective uptake in HepG2 cells | High fluorescence signal in tumors | No weight loss or histological toxicity in liver, spleen, kidney; reduced DOX-induced hepatic toxicity |
| **26** | N1S1 rat liver tumor | ASGPR | Stannous-doped Alginate-PEI-Dox NPs | 100–200 nm; −26 mV; Dox loading: ~13.4%; Encapsulation: ~63%; Sn: ~43 µg/mg | Two-step: 1) Galactose ring-opening; 2) Dropwise addition to PEI-coated NPs | 99m-Tc-based gamma imaging; Infrared (IR) Thermal Imaging | Higher in tumors | Tumor areas reached ~62°C vs. ~42°C in normal liver during RF | Safe at applied RFA parameters |
| **29** | HepG2 tumor-bearing mice | ASGPR | Azido-sugar-labeled cells | Confirmed by ESI-MS, $^1$H NMR, $^{13}$C NMR, and FTIR | N-azidoacetyl–succinamide coupling | Cy5 | GalAz > ManAz > PBS | GalAz yielded the highest fluorescence intensity (ex vivo, confocal imaging | Not mentioned |

**Table 3.** Gal-PNPs targeting galectin or β-galactosidase in tumor microenvironment

| Reference | Model | Target | NP type | NP characteristic | Gal conjugation method | Imaging agent | Tumor uptake | Imaging efficacy | Safety |
|---|---|---|---|---|---|---|---|---|---|
| **23** | 4T1 breast cancer xenograft mice | UV-triggered sialic acid-to-galactose surface conversion on tumor cells | Den@5F penta-functional dendrimer | UV-photoactivated | Click reaction (CuAAC) and EDC/NHS amide linkage | Cy5 | Higher in breast cancer cells | Strong signal for Den@5F up to 48h; High S/N ratio; UV enhances targeting | No abnormalities in major organs |
| **33** | Glioblastoma-bearing mice | Galectins | Hydroxyl-terminated PAMAM dendrimers (G4) | 4.53nm; PDI 0.49; ~7–10 mV; ~12 sugars per dendrimer; >99% purity by HPLC | CuAAC click (PEG spacer) | Cy5 | 2.5× uptake vs. non-galactosylated dendrimers | Tumor/contralateral ratio: 7.1 ± 1.7 | Not enter into microglia |
| **30** | HepG2 tumor-bearing mice | β-Galactosidase / Galectin-1 | TPE-Gal self-assembled amphiphilic micromolecule vesicles | ~120 nm (TEM), 157.4 ± 7.69 nm (DLS); PDI: 0.074; −17.1 ± 4.4 mV; Stable in water, PBS, and plasma | CuAAC click chemistry between azide-functionalized TPE and alkyne-propargyl-galactoside, followed by deacetylation. | TPE (blue), DOX (red) | Higher in HepG2 (Tumor) vs L02 (Normal) | CLSM shows TPE+DOX colocalization; Clear and time-dependent signal | No weight loss, negligible hemolysis, and favorable histology of organs post-treatment |
| **32** | Galectin-1–overexpressing human UMUC3 bladder cancer (an orthotopic murine model) | Galectin-1 | Galactodendritic unit (G1) with $^{18}F$ | High radiochemical purity (99%), with a radiochemical yield of 45%, and strong binding affinity ($K_d$ = 0.067 ± 0.01 mM) to galectin-1 | Di-nucleophilic substitution of triazine core with galactose | $^{18}F$ (PET/CT scan) | High in alectin-1(+) tumors | High PET signal in tumor vs. non-tumor tissues ($SUV_{mean}$: 43.5 ± 4.2 vs. 2.0 ± 0.4); better performance than $^{18}F$-FDG standard tracer ($SUV_{mean}$: 10.5 ± 2.3) | Not mentioned |

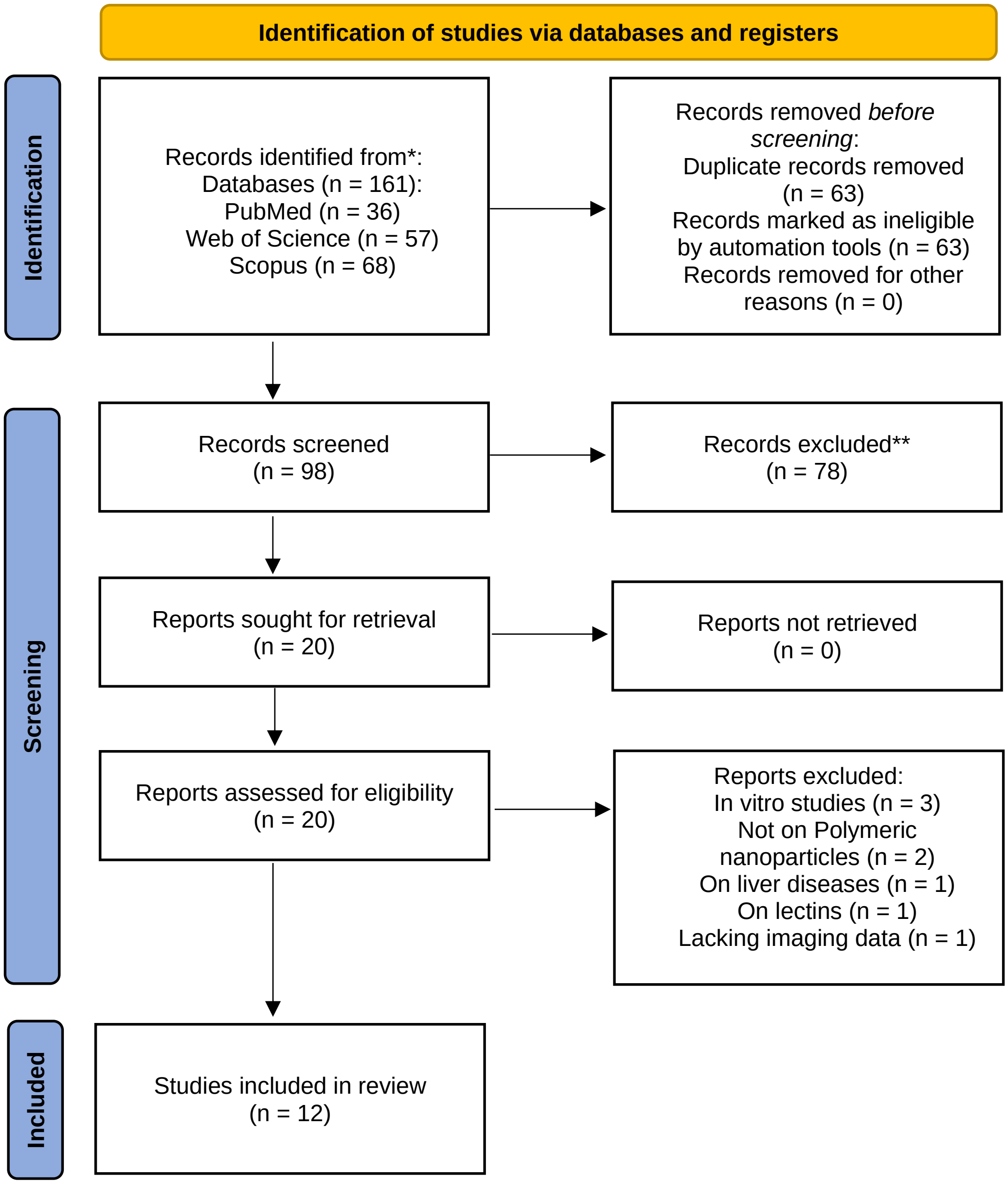


**Figure 1.** PRISMA flow chart illustrates the study selection steps

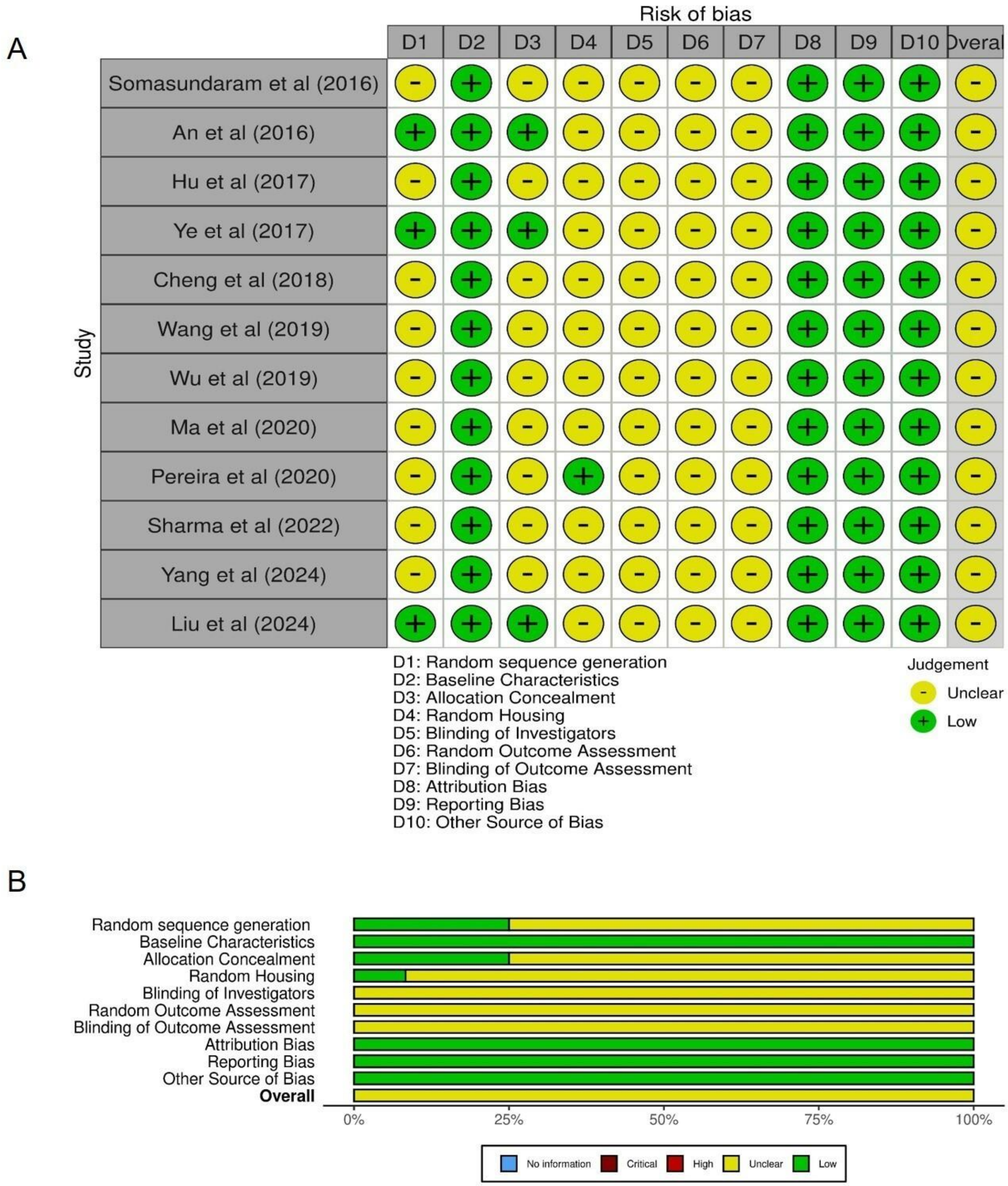


**Figure 2.** Risk of bias assessment for included studies based on the SYRCLE risk of bias tool for animal studies. Studies were assessed in ten domains (D1–D10), and their assessment is shown as low risk (green), uncertain risk (yellow), or high risk (red). Data are presented in (A) a traffic light diagram and (B) a summary diagram (https://mcguinlu.shinyapps.io/robvis/)